Accepted Manuscript

Ballistic performance of Kevlar fabric impregnated with nanosilica/PEG shear thickening fluid

A. Khodadadi, Gh Liaghat, S. Vahid, A.R. Sabet, H. Hadavinia

PII: S1359-8368(18)30909-0

DOI: https://doi.org/10.1016/j.compositesb.2018.12.121

Reference: JCOMB 6450

To appear in: *Composites Part B*

Received Date: 22 March 2018

Revised Date: 19 December 2018

Accepted Date: 29 December 2018

Please cite this article as: Khodadadi A, Liaghat G, Vahid S, Sabet AR, Hadavinia H, Ballistic performance of Kevlar fabric impregnated with nanosilica/PEG shear thickening fluid, *Composites Part B* (2019), doi: https://doi.org/10.1016/j.compositesb.2018.12.121.

Ballistic performance of Kevlar fabric impregnated with nanosilica/PEG shear thickening fluid

A. Khodadadi[1], Gh. Liaghat[1, 2]*, S. Vahid[2], A. R. Sabet[3], H. Hadavinia[2]
[1]Department of Mechanical Engineering, Tarbiat Modares University, 14115-141, Tehran, Iran
[2]School of Mechanical & Automotive Engineering, Kingston University, London, England
[3]Iran Polymer and Petrochemical institute, Tehran, Iran
* Corresponding author, Ghlia530@modares.ac.ir and G.Liaghat@kingston.ac.uk

Abstract

This study presents the response of fiber reinforced composite material composed of woven Kevlar fabric impregnated with a colloidal shear thickening fluid (STF) under high velocity impact loading. The STF was made by dispersing silica nanoparticles at 15, 25, 35 and 45 wt.% loading in polyethylene glycol. The effects of silica nanoparticle loading on energy absorption and ballistic limit were studied experimentally. Rheological results revealed that shear thickening occurred at all four nanosilica loading and higher loading showing the higher shear thickening at lower shear rate. SEM images confirmed good dispersion of nanosilica particles in the suspension. The results of the pull out test show that by increasing nanosilica loading, the force required to pull the yarn out from the fabric impregnated by STF increases. Impact resistance performance of Kevlar fabric is significantly enhanced due to the presence of STF. Although high velocity impact results show that by increasing nanosilica loading, the energy absorption of composites increases, but in high loading of nanosilica, the effectiveness of STF decreases. For further investigation, the energy absorption at the ballistic limit was normalized by the areal density of the neat and impregnated fabrics to give the specific energy absorption (SEA). It is found that the SEA of 15 wt.% nanosilica loading is lower compared to the neat fabric. Also the highest SEA turn out in the case of 35 wt.% STF/Kevlar composites in which the SEA is 2.3 times larger than those of the neat fabric.

Keywords:

High velocity impact, Shear thickening fluid, Nanosilica loading, Kevlar fabric, Nanocomposites.

1. Introduction

Body armors are mainly of two types, namely hard armor and soft armor [1]. Hard body armors are used to ensure protection against high speed projectiles. Metal or ceramic plates are inserted between layers of fabrics to achieve this goal. Consequently hard armors are heavy which restricts the movements of body parts of the wearer [1, 2]. On the contrary, flexible armor or soft armor is mainly used for body protection and provide protection from ballistic threats without significantly limiting the mobility of the wearer. High strength and toughness fabrics such as Kevlar, Twaron and Spectra and composites made from these fabrics are usually used as soft body armor [3, 4]. During the last decade numerous researches have been carried out on the high velocity impact on high strength fabric structures [5-8].

Polymer nanocomposites (PNCs) are advanced engineering materials in which nanoscale fillers, are dispersed in a polymer matrix in order to improve the performance properties of the polymer [9]. Polymer nanocomposites have nano-sized fillers such as carbon nanotube [10], graphene [11-14], titania (TiO_2) [15], or lignin [16] embedded inside the polymer matrix including epoxy [17, 18], polystyrene, polypropylene. The unique structures of PNCs make them possess unique properties when compared to the pure polymers. Therefore, different researches have been conducted on Polymer nanocomposites [19-25], and these materials have been widely used in different fields, such as biological [26, 27], electronics [28-30], electromagnetic [31] and aerospace.

One of the nanocomposite materials taken up by the researchers to improve the impact resistance of fabrics is shear thickening fluid (STF) nanocomposite. STF is generally composed of stabilized dispersions of concentrated rigid nanosilica particles in a polymer fluid [32-34]. Adding shear thickening fluid (STF) nanocomposite to a fabric induces little

increase in the thickness, weight and stiffness of the fabric and improves its impact resistance performance [35, 36]. A lot of research have been conducted on the stab resistance and ballistic performance of STF impregnated (STF-treated) fabric composite [35, 37-44]. Cao et al. [45] used an Split Hopkinson Pressure Bar (SHPB) system to test the mechanical properties and energy absorption of the STF/Kevlar composites at high strain rate. They showed that both the strain rate and the modulus of the STF/Kevlar composite have increasing trend with the increase of impact velocity. Besides, the modulus of composite increased with the increasing of the volume fraction of STF. Also the addition of the STF and the increase of the fabric number reduced the energy transfer rate.

The essential physics of the impact mechanism associated with STF impregnation into fabrics is difficult to investigate through experimental means alone. It has been reported that the primary contribution of STF impregnation in high velocity fabric was the increase of friction between yarns in the fabric that resulted in the enhancement of the energy absorption reflected in experimental observations [46]. Alikarami, et al. [47] conducted an experimental investigation on the yarn pull-out test for calculating friction coefficient in fabric samples for three cases: neat, dissolved liquid, and STF-treated fabrics. Comparing the yarn pull-out force values indicates that the STF-treated samples have the highest value and is approximately three times higher than that of the neat sample. Kordani, et al. [48] conducted high velocity impact experiment to STF-Kevlar fabrics and demonstrated that adding STF to Kevlar fabric can slightly improve impact resistance. They showed that increasing the ethanol ratio in the samples reduces the final viscosity and shortens the stability and transition of shear thickening at a high strain rate. In another study, Na et al. [49] have investigated the rate dependent behavior of an STF impregnated fabric, using uniaxial tensile, bias-extension, and picture-frame tests. Feng, et al. [40] studied the effects of fumed silica in shear thickening

fluids at a weight fraction of 20% and submicron silica particles in shear thickening fluids at a weight fraction of 65% on quasi-static stab resistance properties of fabrics impregnated with shear thickening fluids. The results show that aramid fabrics treated with shear thickening fluid exhibit a significant enhancement in quasi-static stab resistance.

The rheological behavior of shear thickening fluids is affected by a variety of parameters. The most important of which are the preparation methods, particles size, type of particles, particles volume fraction, temperature and liquid medium [50-52]. One of the major factors on the rheology of STFs is the particle loading, defined as the fraction of particle weight to the total weight. Since the STF concentration undoubtedly is one of the most important parameters affecting shear thickening phenomena and subsequently on the impact resistance behavior of the STF/Kevlar composites, in the present study, rheological tests have been carried out for the STF at four loading levels of 15, 25, 35 and 45 wt.%. Also yarn pull out test have been done. Afterwards, high velocity impact tests have been conducted for the two and four layer neat and impregnated fabrics and energy absorption and specific energy absorption of the STF/fabric composite have been obtained.

2. Experiments

2.1. Materials

Shear Thickening Fluid. The shear thickening fluid (STF) used in this study is composed of silica nanoparticles suspended in polyethylene glycol, at nanoparticle loadings of 15, 25,35 and 45 wt. %. The average particle diameter, measured by dynamic light scattering is 500 nm. Rheological characterization of this STF confirmed discontinuous shear thickening at a shear rate of approximately $1\text{-}10^2$ s^{-1}.

Kevlar Fabric. The plain-woven fabric used in all composite target was Kevlar style 706 produced by the Hexcel Corporation. The dimension of fabric for impregnation with STF was 140×140 mm^2.

2.2. Sample preparation

Shear Thickening Fluid was prepared by dispersion of 15, 25, 35 and 45 wt. % Aerosil OX50 fumed silica particles with 500 nm average particle size, in polyethylene glycol (PEG). Particles were dispersed in the polyethylene glycol, through a combination of shear mixing homogenizer at 8000 RPM and ultra-sonication (Bandelin HD3200).

The impregnation of the Kevlar fabric yarns for the preparation of the STF-Kevlar composite target, is facilitated by diluting STF in ethanol at a 1:2 volume ratio and individual fabric layers were soaked in the diluted STF for 1 min. After impregnation with the ethanol/STF mixture, fabric layers were heated in an oven at 70°C for 20 minutes to remove the ethanol. Fig. 1 shows the major steps in fabricating the colloidal suspension and impregnation of the fabric. The areal densities of the impregnated fabric targets were determined by weighing the different fabric ply systems before and after impregnation with STF. Characteristics of the neat and impregnated fabric are presented in Table 1.

2.3. Scanning Electron Microscopy studies

SEM studies were carried out using a JEOL JSM 5800 scanning electron microscope manufactured by Gen Tech. The SEM samples were prepared by uniformly spreading the as-prepared STF samples on a double-sided carbon tape and coated with gold/palladium to prevent charge buildup by the electron absorption. Note that most of the PEG component of the STF evaporates under high vacuum and electron beam irradiation, so the images will show only dry silica where STF existed under ambient conditions.

2.4. Rheological behaviors

The rheological behaviors of 15, 25, 35 and 45 wt% STF samples were investigated using an Anton Paar MCR501 stress-controlled rheometer with a torque range from 0.01 µN.m to 300 mN.m with a torque resolution of 0.1 nN.m and Shear Rate from 0/01 to 2000 1/s.

2.5. Yarn pull out

In order to investigate the effect of friction between Kevlar yarns, pull out test was conducted on neat and STF impregnated fabric. Tests were conducted on the tensile testing machine Santam 6025. Single yarn from each specimen was fixed in the upper grip of the tensile testing machine and the lower part of the specimen was mounted on a grip.

2.6. High velocity impact tests

High-velocity impact tests were carried out using a gas gun on two and four-layer neat Kevlar fabric and on STF/Kevlar composite at four different levels of nanosilica loading (15, 25, 35 and 45 wt.% STF) in a velocity range of 40 to 160 m/s. Three tests were carried out at each velocity, and average with standard deviation are reported here.

All the tests were performed at room temperature. The gun was sighted on the target center. The exact impact velocity of each projectile was measured with a chronograph immediately before and after impacting the target. Schematic of gas-gun set up is shown in Fig. 2. The specimens comprised of two and four plies with dimension of 140×140 mm. The projectile is hemispherical steel 4330 with diameter 8.74 mm and mass 11.18 g. The energy absorbed by the specimens during the penetration can be calculated from the initial velocity and residual velocity.

$$E_i = \frac{1}{2} m_P V_i^2 \quad (1)$$

$$E_r = \frac{1}{2} m_P V_r^2 \quad (2)$$

$$E_P = \frac{1}{2} m_P (V_i^2 - V_r^2) \quad (3)$$

Where E_P (J) represents the dissipated energy during the impact process, m_P (kg) is mass of the projectile, V_i (m/s) is projectile initial velocity, and V_r (m/s) is residual velocity.

Slipping and pulling out of the specimens from the fixture, is avoided by putting sandpaper on both sides of the specimens and the framework. All 4 sides of the specimens were constrained completely as shown in Fig. 3.

3. Results and discussion

3.1. Rheological properties

The rheological behavior of STF at four different nanosilica loading (15, 25, 35 and 45 wt. %) is presented in Fig. 4. For all STF specimens the response of viscosity to shear rate is non-Newtonian and completely nonlinear and both shear thinning and shear thickening behavior are observed. Shear thinning occurs at low shear rates followed by shear thickening at high shear rates. Shear thickening phenomenon can be described by the transition of the nanoparticles from an equilibrium state to agglomerated state and as it is shown, the rheology of STF considerably depends on the volume fraction of the suspension. As the magnitude of shear rate increases to a critical value, the viscosity suddenly increases. This critical shear rate value decreases by increasing the nanosilica loading. The increase in nanoparticles inside the suspension restricts relative movement of fluid layers to one another and thus increases the viscosity. The critical shear rates are 100 s^{-1} for the STF having nanosilica loading of 15

wt. % and less than 10 s^{-1} for the STF with nanosilica loading of 45 wt. %. Viscosity curve of the STF shifted upward on the graph by increasing the nanosilica loading. In other words, the higher particle loading results in a higher initial viscosity and exhibits a greater increase in viscosity. Fig. 5 shows the peak value of viscosity for STFs with different nanosilica loading. The peak loads of STF containing nanosilica loading of 25, 35 and 45 wt.% are 30, 136 and 469 times greater than STF containing 15 wt.% nanosilica, respectively.

The primary theory which presented the mechanism of the thickening was hydro-cluster theory [53, 54]. This theory stated that as the shear rate increases, the microstructure of the colloidal dispersions changes and the hydrodynamic loads overcome the interparticles loads, which leads to the formation of particle clusters and ultimately the increase of suspension viscosity. By increasing the solid content, hydrodynamic forces dominate the suspension which causes the hydro-clusters to be formed more quickly. As well as hydro-clustering approach, the contribution of contact forces is suggested in recent studies known as contact rheology model [55, 56]. Denn et al. [57] stated that the hydro-clustering approach dominates the suspensions at low shear rates due to contactless rheology, but the contact forces are very effective for the jamming point where the particles contact each other at high shear rates. Beyond a critical point, contact forces generate force networks that dominate thickening where the hydrodynamic interactions are insufficient. Nanosilica loading plays an important role in contact rheology due to increase possibility of the contacted microstructure by increasing concentration particles in the suspension [58].

3.2. Microstructural analysis

According to the images of the silica/Kevlar composite fabric, fibers are covered with STF and nanoparticles located between them. With the increase of STF concentration, the amount

of STF between the fibers increases and the gaps between the fibers fills more uniformly. The surface morphologies of the silica/ Kevlar composite fabric at different magnification are shown in SEM images in Fig. 6 for the 35 wt. % sample. It can be seen that the gaps between yarns at yarn crossover areas are well coated by the STF.

3.3. Yarn pull out test

Previous studies have shown that fabric impregnated STF demonstrated increase in inter-yarn friction and this is the main cause of performance improvement of STF [59]. Some experimental and numerical studies have shown that modification of the frictional properties of the fabric can affect the yarn pull-out behavior. Increase in yarn pull-out force, can also be a major factor to the overall energy dissipated by a fabric [60].

It is also shown that inter-yarn friction of the fabrics greatly alters, with respect to the particle mass fraction in shear thickening fluids [61]. The concentration of additive nanoparticles in STF is effective in increasing the pull-out force. This means the inter-yarn friction increases by increasing particle loading. The influence of the impregnation on inter-yarn friction is investigated by yarn pull-out tests using a tensile testing machine. Yarn pull-out tests were carried out for neat and impregnated Kevlar fabrics.

Fig. 7 shows the corresponding fiber pull-out force versus displacement for neat, 15 wt. %, 25 wt. %, 35 wt. % and 45 wt. % STF/Kevlar composite. The tests were carried out at 100 mm/min. At the beginning of the testing, the pull-out force increases as the yarn is progressively straightened until the peak point is reached. When the pull-out force surpasses the static friction limit, it drops gradually from the peak point and oscillates while the free end of the yarn passes each crossing yarn. The figure shows considerable higher attaining

frictional load for the STF impregnated yarn. Table 2 presents the peak load for all specimens. Therefore, by increasing nanosilica loading, the peak load of pull-out increases. This increase is the result of positioning of the additive particles between the fibers. Interlocking of the fibers increases due to the additive particles intercalated between the fibers and yarns [62]. So when nanoparticle loading increases, more pull-out forces are required to overcome the inter-yarn friction in the fabrics. Other notable result from the pull-out test reveals much gradual drop in load after attaining the peak load. Both behaviors are directly attributed to effect of silica particles presence on the yarn as a result of STF impregnation. Other notable result from the pull-out test is the stiffer response (steep initial rise) by STF impregnated fabric compared to neat fabric.

3.4. High velocity impact tests

3.4.1. Ballistic limit

High-velocity impact test was conducted on two and four-layer neat and STF/Kevlar composite with STF containing 15, 25, 35 and 45 wt. % fumed silica in polyethylene glycol (PEG) medium. The tests were conducted at different impact velocities to find ballistic limit (V_{50}) of each sample by controlling the gas pressure in the gas gun. V_{50} is ballistic limit velocity and it is defined as the average of equal number of highest partial penetration velocities and lowest complete penetration velocities of a projectile and a target combination, which occur within a specified velocity range. In other words, V_{50} defines incident impact velocity at which there is 50% probability of partial penetration and 50% probability of perforation. A minimum of three partial and three complete penetration velocities are used to compute V_{50} [63].

The high velocity impact test results are presented in Table 3 for all samples. Results shows enhancement in ballistic performance in term of lower residual velocity for two and four-layer STF impregnated specimens compared to corresponding neat Kevlar fabric. It means STF impregnated fabrics showing better impact resistance compared to neat fabrics. Better performance can be attributed to the higher number of fibers remaining in contact with the projectile surface area during penetration and perforation of the STF impregnated fabric. The higher number of fibers in contact with the projectile surface area can be directly related to friction enhancement associated with the STF impregnated on the fabric.

Fig. 8 shows that the ballistic limit of two and four-layer neat and STF/Kevlar composites. It is shown that ballistic limit increases by increasing nanosilica loading from 15 wt.% to 35 wt.%. After which, variation of ballistic limit disappear and ballistic limits of 35 and 45 wt.% STF are very close to each other. Hence, although STF enhances the energy absorption, there is an optimal nanosilica loading.

With the increase of particles loading in the STF up to 35 wt.%, the maximum ballistic limit of the Kevlar/STF composite or, in other words, the impact resistance performance of the composite increases significantly. The increase of nanosilica loading leads to higher friction between fibers and between yarns, keeping better fibers arrangement, more consistent, uniform and integrated fabric coating, less gaps, less yarns and fibers sliding, extracting and windowing under impact loading and better stress distribution in the Kevlar/STF composite. On the other hand, by increasing nanosilica loading to 45 wt.%, the effectiveness of STF vanishes in high velocity impact due to the stress concentration between yarns and layers which is created in this high loading of nanosilica.

3.4.2. Specific Energy absorption

Fig. 9 shows the energy absorption of two and four-layer neat and impregnated fabrics with nanosilica loading of 15, 25, 35 and 45 wt.% at ballistic limit velocity. It is shown that the energy absorption of STF/Kevlar composite increases as the nanosilica loading increases. Energy absorption increases about 90%, 286.4%, 605% and 623% for 15, 25, 35 and 45 wt. % STF, respectively comparing to four layer neat fabric. This values for 2 layer specimens are 117.9%, 300%, 611.1% and 636.3%.

It can be seen that by increasing nanosilica loading, the absorbed energy in the sample increases. On the other hand, the weight of the samples is also increased by impregnation. To evaluate the effect of the weight gain and energy absorption, specific energy absorption (SEA) has been evaluated. SEA is the energy absorbed by the sample to its areal density. Fig. 10 shows the specific energy absorption of each fabric samples that is calculated from equation 4.

$$\text{specific energy absorption} = \frac{\frac{1}{2} m V_{50}^{2}}{\text{Areal density}} \quad (4)$$

The specific energy absorption of neat fabrics is considered as a reference. As can be seen, the sample of two and four layer impregnated with STF containing 35 wt.% nanoparticles has the highest SEA. Although this specimen has higher weight comparing to neat fabric, but the amount of energy absorbed is much higher, and therefore the SEA is the highest. Therefore, the use of a STF/composite with 35 wt.% nanosilica, is reasonable. The SEA of four layer fabric impregnated with 35 wt. % STF is 24.28 Jm^2/Kg which is nearly equal to two times greater than the SEA of a neat four layer fabric. Also, STF/Kevlar composite containing 15 wt. % nanosilica, has the lowest SEA compared to the neat fabric. This indicates that impregnating the fabric by 15 wt.% STF is not effective, even though it increases the energy

absorption of neat fabrics. As can be seen the SEA of four layer STF/Kevlar composite containing 45 wt.% nanosilica is 22.31 Jm^2/Kg which shows 8% decrease comparing to 35 wt.% STF. Too high friction may reduce yarn movement leading to stress concentration between yarns resulting in reduced impact performance.

According to Fig. 10, the highest SEA is associated with 4-layer Kevlar fabric with STF containing 35 wt.% nanosilica materials. The reason is the fact that as the number of layers increases, better interactions between the layers occurs and fabric dissipates energy more efficiently after projectile impact.

The STF reinforcement factor is proposed to provide a better measure of the ballistic performance of impregnated fabrics comparing to neat fabric. It is the ratio of the SEA of the impregnated fabric to that of the respective neat one.

$$\text{Reinforcement factor} = \frac{\text{SEA of impregnated fabric}}{\text{SEA of neat fabric}} \quad (5)$$

Fig. 11 shows the reinforcement factors for two and four-layer STF/Kevlar composite containing various nanosilica loading. By definition, a neat fabric has a reinforced factor of one. The Reinforcement factor shows that the highest improvements in the specific ballistic energy are 126% for two-layer and 129% for four-layer composite at 35 wt.% STF.

3.4.3. Fabric deformations

The high velocity impact tests were performed to explore fabric impact resistance and the mechanisms that are contributed in energy absorption of neat and impregnated Kevlar fabric. Three mechanisms of fiber/yarn breakage (fracture), slippage (windowing) and yarn pull out are the most important factors affecting fabric impact resistance. Fig. 12 shows perforated samples including neat and 15, 25, 35 and 45 wt.% STF/Kevlar composites after high

velocity impact tests. As can be seen in the figure, the global transverse deflection shapes exhibit similar behavior for both neat fabric and STF impregnated fabrics. However, the local fabric structures in the impact region of STF impregnated fabric are well maintained, while they are significantly distorted for the neat fabric. Moreover in some cases when projectile penetrates the neat fabric, yarns are pushed aside within the fabric without significant fiber breakage under impact load. This phenomenon is called windowing effect. Although primary yarns in the center of impact strained in the neat fabric, rest of the fabric (secondary yarns) remains almost undisturbed. This brings out the inability of the neat Kevlar fabric structure in engaging secondary yarns in energy sharing during impact. As a result, energy dissipation along the fabric remains low and the impact resistance performance decreases. Notably, significant yarn pull-out is observed at the impact point for the neat fabric.

In the fabrics impregnated by STF, yarn pull-out is hardly observed, especially at higher nanosilica loading, and the damage zone are becoming much smaller. The increased frictional properties induced by STF impregnation restrict the movement of the yarns, thus encouraging neighboring yarns to arrest the projectile. The STF impregnated fabrics are able to maintain their weave integrity during the impact process. As shown for in Fig. 12, for fabric composites made impregnated with STF with 35 and 45 wt. % nanoparticles, no yarn pull out is observed. In images taken with a high speed camera, it has been shown that in neat fabric specimens, a number of fibers are pulled out of the fabric and move with the bullet.

4. Conclusions

High-velocity impact test was conducted on two and four-layer neat and STF/Kevlar composite containing 15, 25, 35 and 45 wt. % nanosilica in polyethylene glycol (PEG) medium and the effect of nanosilica loading was investigated. The energy absorption of neat

fabric increases by impregnating the fabric with STF. It was found that there is an optimum nanosilica loading that beyond it the increase rate changes. By increasing of nanosilica loading in STF from 15 to 35 wt.%, the performance of composite is extraordinary and improvement rate is intense, but improvement rate decreases and a little improvement is shown from 35 to 45 wt.% STF. The most effective performance turn out in the case of 35 wt.% STF/Kevlar composites in which the specific energy absorption is the highest between composites containing 15, 25 and 45 wt. % nanosilica. Yarn pull-out tests were also carried out neat and impregnated Kevlar fabrics. By increasing the nanoparticles loading a notable increase of pull-out force was shown, which indicates the effect of friction. On the other hand, by increasing nanosilica loading from 35 to 45 wt.%, the energy absorption of composite doesn't vary significantly which means the yarn pull-out force doesn't affect the energy absorption directly and shows the different effect of friction in static and impact forces. It is found that by increasing the number of layers, better interactions between the layers occurs and fabric dissipates energy more efficiently. In the fabrics impregnated by STF, yarn pull-out is hardly observed, especially at higher nanosilica loading, and the damage zone are becoming much smaller.

ACKNOWLEDGMENTS

The authors are grateful to the Tarbiat Modares University (TMU) for their financial support.

References

[1] Srivastava A, Majumdar A, Butola B. Improving the impact resistance of textile structures by using shear thickening fluids: a review. Critical Reviews in Solid State and Materials Sciences. 2012;37(2):115-29.

[2] Ahmadi H, Liaghat G, Sabouri H, Bidkhouri E. Investigation on the high velocity impact properties of glass-reinforced fiber metal laminates. Journal of Composite Materials. 2013;47(13):1605-15.

[3] Nilakantan G, Merrill RL, Keefe M, Gillespie Jr JW, Wetzel ED. Experimental investigation of the role of frictional yarn pull-out and windowing on the probabilistic impact response of Kevlar fabrics. Composites Part B: Engineering. 2015;68:215-29.

[4] Duan Y, Keefe M, Bogetti T, Cheeseman B. Modeling friction effects on the ballistic impact behavior of a single-ply high-strength fabric. International Journal of Impact Engineering. 2005;31(8):996-1012.

[5] Shanazari H, Liaghat G, Hadavinia H, Aboutorabi A. Analytical investigation of high-velocity impact on hybrid unidirectional/woven composite panels. Journal of Thermoplastic Composite Materials. 2017;30(4):545-63.

[6] Zhu D, Vaidya A, Mobasher B, Rajan SD. Finite element modeling of ballistic impact on multi-layer Kevlar 49 fabrics. Composites Part B: Engineering. 2014;56:254-62.

[7] Mamivand M, Liaghat G. A model for ballistic impact on multi-layer fabric targets. International Journal of Impact Engineering. 2010;37(7):806-12.

[8] Kędzierski P, Popławski A, Gieleta R, Morka A, Sławiński G. Experimental and numerical investigation of fabric impact behavior. Composites Part B: Engineering. 2015;69:452-9.

[9] Zhao J, Wu L, Zhan C, Shao Q, Guo Z, Zhang L. Overview of polymer nanocomposites: Computer simulation understanding of physical properties. Polymer. 2017; 133;272-87.

[10] He Y, Yang S, Liu H, Shao Q, Chen Q, Lu C, et al. Reinforced carbon fiber laminates with oriented carbon nanotube epoxy nanocomposites: Magnetic field assisted alignment and cryogenic temperature mechanical properties. Journal of colloid and interface science. 2018;517:40-51.

[11] Guo Y, Xu G, Yang X, Ruan K, Ma T, Zhang Q, et al. Significantly enhanced and precisely modeled thermal conductivity in polyimide nanocomposites with chemically modified graphene via in situ polymerization and electrospinning-hot press technology. Journal of Materials Chemistry C. 2018;6(12):3004-15.

[12] Liu H, Huang W, Yang X, Dai K, Zheng G, Liu C, et al. Organic vapor sensing behaviors of conductive thermoplastic polyurethane–graphene nanocomposites. Journal of Materials Chemistry C. 2016;4(20):4459-69.

[13] Wang X, Liu X, Yuan H, Liu H, Liu C, Li T, et al. Non-covalently functionalized graphene strengthened poly (vinyl alcohol). Materials & Design. 2018;139:372-9.

[14] Liu H, Dong M, Huang W, Gao J, Dai K, Guo J, et al. Lightweight conductive graphene/thermoplastic polyurethane foams with ultrahigh compressibility for piezoresistive sensing. Journal of Materials Chemistry C. 2017;5(1):73-83.

[15] Cui X, Zhu G, Pan Y, Shao Q, Dong M, Zhang Y, et al. Polydimethylsiloxane-titania nanocomposite coating: Fabrication and corrosion resistance. Polymer. 2018;138:203-10.

[16] Ma Y, Lv L, Guo Y, Fu Y, Shao Q, Wu T, et al. Porous lignin based poly (acrylic acid)/organo-montmorillonite nanocomposites: swelling behaviors and rapid removal of Pb (II) ions. Polymer. 2017;128:12-23.

[17] Wang C, Zhao M, Li J, Yu J, Sun S, Ge S, et al. Silver nanoparticles/graphene oxide decorated carbon fiber synergistic reinforcement in epoxy-based composites. Polymer. 2017;131:263-71.

[18] Zhang Y, Zhao M, Zhang J, Shao Q, Li J, Li H, et al. Excellent corrosion protection performance of epoxy composite coatings filled with silane functionalized silicon nitride. Journal of Polymer Research. 2018;25(5):130.

[19] Li Y, Wu X, Song J, Li J, Shao Q, Cao N, et al. Reparation of recycled acrylonitrile-butadiene-styrene by pyromellitic dianhydride: reparation performance evaluation and property analysis. Polymer. 2017;124:41-7.

[20] Wang YP, Zhou P, Luo SZ, Guo S, Lin J, Shao Q, et al. In situ polymerized poly (acrylic acid)/alumina nanocomposites for Pb2+ adsorption. Advances in Polymer Technology. 2018; doi: 10.1002/adv.21969.

[21] Zhou P, Wang S, Tao C, Guo X, Hao L, Shao Q, et al. PAA/alumina composites prepared with different molecular weight polymers and utilized as support for nickel‐based catalyst. Advances in Polymer Technology. 2018; doi: 10.1002/adv.21908.

[22] Cheng C, Fan R, Wang Z, Shao Q, Guo X, Xie P, et al. Tunable and weakly negative permittivity in carbon/silicon nitride composites with different carbonizing temperatures. Carbon. 2017;125:103-12.

[23] Hu Z, Shao Q, Huang Y, Yu L, Zhang D, Xu X, et al. Light triggered interfacial damage self-healing of poly (p-phenylene benzobisoxazole) fiber composites. Nanotechnology. 2018;29(18):185602.

[24] Wang C, Mo B, He Z, Xie X, Zhao CX, Zhang L, et al. Hydroxide ions transportation in polynorbornene anion exchange membrane. Polymer. 2018;138:363-8.

[25] Wang C, Wu Y, Li Y, Shao Q, Yan X, Han C, et al. Flame‐retardant rigid polyurethane foam with a phosphorus‐nitrogen single intumescent flame retardant. Polymers for Advanced Technologies. 2018;29(1):668-76.

[26] Shi Z, Shi X, Ullah MW, Li S, Revin VV, Yang G. Fabrication of nanocomposites and hybrid materials using microbial biotemplates. Advanced Composites and Hybrid Materials. 2018;1(1):79-93.

[27] Kiprono S, Ullah M, Yang G. Surface engineering of microbial cells: strategies and applications. Eng Sci. 2018;1:33-45.

[28] Sun K, Xie P, Wang Z, Su T, Shao Q, Ryu J, et al. Flexible polydimethylsiloxane/multi-walled carbon nanotubes membranous metacomposites with negative permittivity. Polymer. 2017;125:50-7.

[29] Sun K, Fan R, Zhang X, Zhang Z, Shi Z, Wang N, et al. An overview of metamaterials and their achievements in wireless power transfer. Journal of Materials Chemistry C. 2018;6(12):2925-43.

[30] Wu Z, Gao S, Chen L, Jiang D, Shao Q, Zhang B, et al. Electrically insulated epoxy nanocomposites reinforced with synergistic core–shell SiO2@ MWCNTs and montmorillonite bifillers. Macromolecular Chemistry and Physics. 2017;218(23):1700357.

[31] Gu H, Zhang H, Lin J, Shao Q, Young DP, Sun L, et al. Large negative giant magnetoresistance at room temperature and electrical transport in cobalt ferrite-polyaniline nanocomposites. Polymer. 2018;143:324-30.

[32] Park Y, Kim Y, Baluch AH, Kim C-G. Empirical study of the high velocity impact energy absorption characteristics of shear thickening fluid (STF) impregnated Kevlar fabric. International Journal of Impact Engineering. 2014;72:67-74.

[33] Lee YS, Wetzel ED, Wagner NJ. The ballistic impact characteristics of Kevlar® woven fabrics impregnated with a colloidal shear thickening fluid. Journal of materials science. 2003;38(13):2825-33.

[34] Majumdar A, Butola BS, Srivastava A. An analysis of deformation and energy absorption modes of shear thickening fluid treated Kevlar fabrics as soft body armour materials. Materials & Design. 2013;51:148-53.

[35] Gürgen S, Kuşhan MC. The stab resistance of fabrics impregnated with shear thickening fluids including various particle size of additives. Composites Part A: Applied Science and Manufacturing. 2017;94:50-60.

[36] Wagner N, Wetzel ED. Advanced body armor utilizing shear thickening fluids. Google Patents; 2009.

[37] Decker M, Halbach C, Nam C, Wagner N, Wetzel E. Stab resistance of shear thickening fluid (STF)-treated fabrics. Composites science and technology. 2007;67(3-4):565-78.

[38] Hassan TA, Rangari VK, Jeelani S. Synthesis, processing and characterization of shear thickening fluid (STF) impregnated fabric composites. Materials Science and Engineering: A. 2010;527(12):2892-9.

[39] Kang TJ, Hong KH, Yoo MR. Preparation and properties of fumed silica/Kevlar composite fabrics for application of stab resistant material. Fibers and Polymers. 2010;11(5):719-24.

[40] Feng X, Li S, Wang Y, Wang Y, Liu J. Effects of different silica particles on quasi-static stab resistant properties of fabrics impregnated with shear thickening fluids. Materials & Design. 2014;64:456-61.

[41] Li W, Xiong D, Zhao X, Sun L, Liu J. Dynamic stab resistance of ultra-high molecular weight polyethylene fabric impregnated with shear thickening fluid. Materials & Design. 2016;102:162-7.

[42] Park JL, Yoon BI, Paik JG, Kang TJ. Ballistic performance of p-aramid fabrics impregnated with shear thickening fluid; part I–effect of laminating sequence. Textile Research Journal. 2012;82(6):527-41.

[43] Park JL, Yoon BI, Paik JG, Kang TJ. Ballistic performance of p-aramid fabrics impregnated with shear thickening fluid; Part II–Effect of fabric count and shot location. Textile Research Journal. 2012;82(6):542-57.

[44] Srivastava A, Majumdar A, Butola BS. Improving the impact resistance performance of Kevlar fabrics using silica based shear thickening fluid. Materials Science and Engineering: A. 2011;529:224-9.

[45] Cao S, Chen Q, Wang Y, Xuan S, Jiang W, Gong X. High strain-rate dynamic mechanical properties of Kevlar fabrics impregnated with shear thickening fluid. Composites Part A: Applied Science and Manufacturing. 2017;100:161-9.

[46] Gürgen S, Kuşhan MC. The ballistic performance of aramid based fabrics impregnated with multi-phase shear thickening fluids. Polymer Testing. 2017;64:296-306.

[47] Alikarami S, Kordani N, SadoughVanini A, Amiri H. Effect of the yarn pull-out velocity of shear thickening fluid-impregnated Kevlar fabric on the coefficient of friction. Journal of Mechanical Science and Technology. 2016;30(8):3559-65.

[48] Kordani N, Vanini AS. Optimizing the ethanol content of shear thickening fluid/fabric composites under impact loading. Journal of Mechanical Science and Technology. 2014;28(2):663-7.

[49] Na W, Ahn H, Han S, Harrison P, Park JK, Jeong E, et al. Shear behavior of a shear thickening fluid-impregnated aramid fabrics at high shear rate. Composites Part B: Engineering. 2016;97:162-75.

[50] Gürgen S, Kuşhan MC, Li W. Shear thickening fluids in protective applications: A review. Progress in Polymer Science. 2017;75;48-72.

[51] Maranzano BJ, Wagner NJ. The effects of particle size on reversible shear thickening of concentrated colloidal dispersions. The Journal of chemical physics. 2001;114(23):10514-27.

[52] Lu Z, Wu L, Gu B, Sun B. Numerical simulation of the impact behaviors of shear thickening fluid impregnated warp-knitted spacer fabric. Composites Part B: Engineering. 2015;69:191-200.

[53] Lim AS, Lopatnikov SL, Wagner NJ, Gillespie JW. Investigating the transient response of a shear thickening fluid using the split Hopkinson pressure bar technique. Rheologica acta. 2010;49(8):879-90.

[54] Lim AS, Lopatnikov SL, Wagner NJ, Gillespie Jr JW. Phenomenological modeling of the response of a dense colloidal suspension under dynamic squeezing flow. Journal of Non-Newtonian Fluid Mechanics. 2011;166(12-13):680-8.

[55] Lin NY, Guy BM, Hermes M, Ness C, Sun J, Poon WC, et al. Hydrodynamic and contact contributions to continuous shear thickening in colloidal suspensions. Physical review letters. 2015;115(22):228304.

[56] Peters IR, Majumdar S, Jaeger HM. Direct observation of dynamic shear jamming in dense suspensions. Nature. 2016;532(7598):214.

[57] Mari R, Seto R, Morris JF, Denn MM. Shear thickening, frictionless and frictional rheologies in non-Brownian suspensions. Journal of Rheology. 2014;58(6):1693-724.

[58] Gürgen S, Li W, Kuşhan MC. The rheology of shear thickening fluids with various ceramic particle additives. Materials & Design. 2016;104:312-9.

[59] Khodadadi A, Liaghat G, Sabet A, Hadavinia H, Aboutorabi A, Razmkhah O, et al. Experimental and numerical analysis of penetration into Kevlar fabric impregnated with shear thickening fluid. Journal of Thermoplastic Composite Materials. 2018;31(3):392-407.

[60] Fahool M, Sabet AR. Parametric study of energy absorption mechanism in Twaron fabric impregnated with a shear thickening fluid. International Journal of Impact Engineering. 2016;90:61-71.

[61] Majumdar A, Butola BS, Srivastava A. Development of soft composite materials with improved impact resistance using Kevlar fabric and nano-silica based shear thickening fluid. Materials & Design (1980-2015). 2014;54:295-300.

[62] McAllister QP, Gillespie Jr JW, VanLandingham MR. The energy dissipative mechanisms of particle-fiber interactions in a textile composite. Journal of Composite Materials. 2014;48(28):3553-67.

[63] Pandya K, Akella K, Joshi M, Naik N. Ballistic impact behavior of carbon nanotube and nanosilica dispersed resin and composites. Journal of Applied Physics. 2012;112(11):113522.

Table 1 Characteristics of neat and impregnated fabrics.

	Samples	Weight (g)	Areal density (kg/m^2)
2 layers	neat Kevlar fabric	9.1	0.464
	Kevlar fabric impregnated with STF (15 wt.% nanosilica)	20.5	1.046
	Kevlar fabric impregnated with STF (25 wt.% nanosilica)	26	1.326
	Kevlar fabric impregnated with STF (35 wt.% nanosilica)	28.3	1.444
	Kevlar fabric impregnated with STF (45 wt.% nanosilica)	30.7	1.627
4 layers	neat Kevlar fabric	18.2	0.928
	Kevlar fabric impregnated with STF (15 wt.% nanosilica)	41	2.092
	Kevlar fabric impregnated with STF (25 wt.% nanosilica)	52	2.652
	Kevlar fabric impregnated with STF (35 wt.% nanosilica)	56.6	2.888
	Kevlar fabric impregnated with STF (45 wt.% nanosilica)	61.4	3.254

Table 2 Quantitative data of peak load extracted from Fig. 6.

Nanosilica particles loading	Peak Load	Increase in peak load (%)
Neat fabric	8.33	-
Kevlar/STF (15 wt.% nanosilica)	10.6	27.2
Kevlar/STF (25 wt.% nanosilica)	13.2	58.5
Kevlar/STF (35 wt.% nanosilica)	16.3	95.7
Kevlar/STF (45 wt.% nanosilica)	18.1	117.3

Table 3 Results for high-velocity impact tests.

Sample	Number of layers	Specimen number	Impact velocity (m/s)	Residual velocity (m/s)	Energy absorption (J)
Neat fabric	2	1	40	28	4.57
	2	2	47	37	4.7
	2	3	52	43	4.79
	4	1	52	27	11.06
	4	2	71	52	13.09
	4	3	80	61	15
STF/Kevlar composite (15 wt.% nanosilica	2	1	46	23	8.89
	2	2	52	33	9.04
	2	3	65	48	10.76
	4	1	75	34	25.03
	4	2	85	49	27.01
	4	3	101	64	34.19
STF/Kevlar composite (25 wt.% nanosilica	2	1	73	42	19.96
	2	2	85	60	20.3
	2	3	91	67	21.23
	4	1	96	45	40.27
	4	2	110	67	42.62
	4	3	122	82	45.69
STF/Kevlar composite (35 wt.% nanosilica	2	1	88	42	33.49
	2	2	99	63	32.66
	2	3	111	79	34.05
	4	1	130	65	70.98
	4	2	142	88	69.55
	4	3	157	104	77.46
STF/Kevlar composite (45 wt.% nanosilica	2	1	90	44	34.4
	2	2	104	68	34.6
	2	3	118	87	35.5
	4	1	135	71	73.7
	4	2	147	92	73.5
	4	3	160	111	74.2

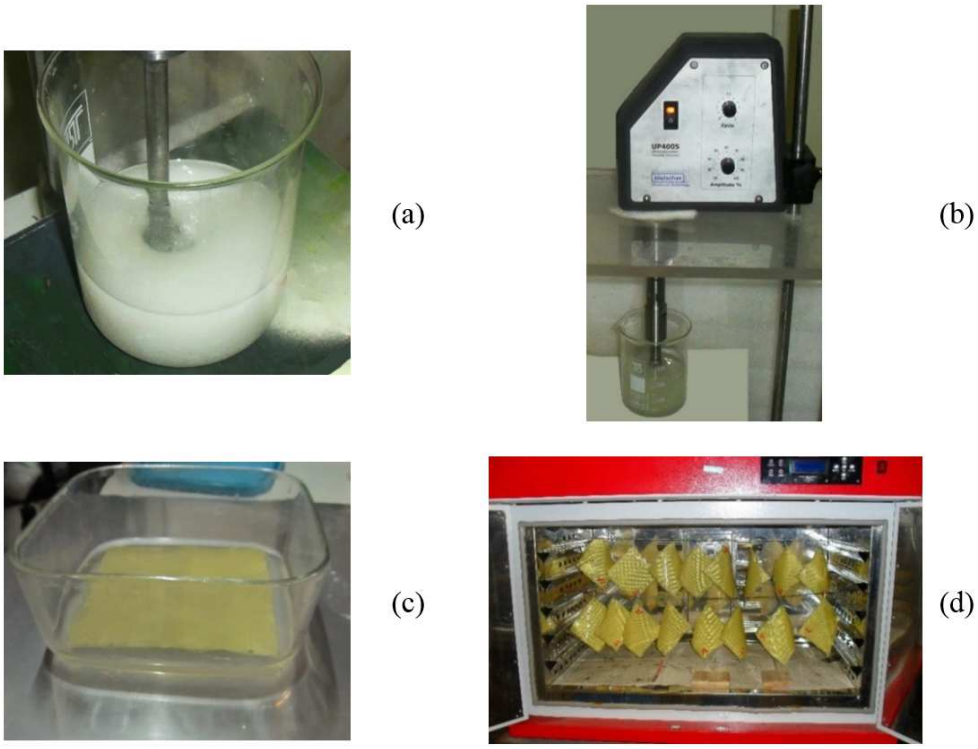

Fig. 1 Steps of the fabric impregnation (a) Homogenization, (b) Sonication, (c) Immersion, (d) Evaporation of ethanol from impregnated fibers.

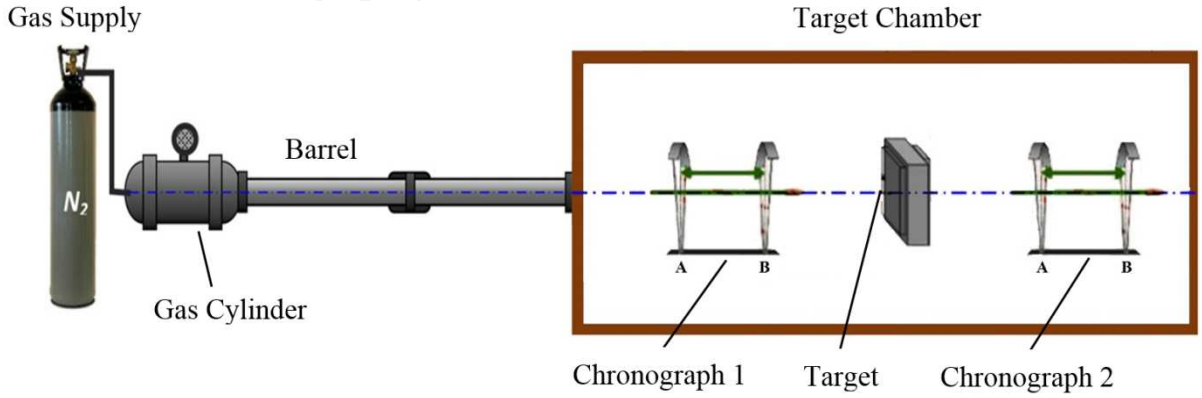

Fig. 2 Schematic set-up of gas-gun.

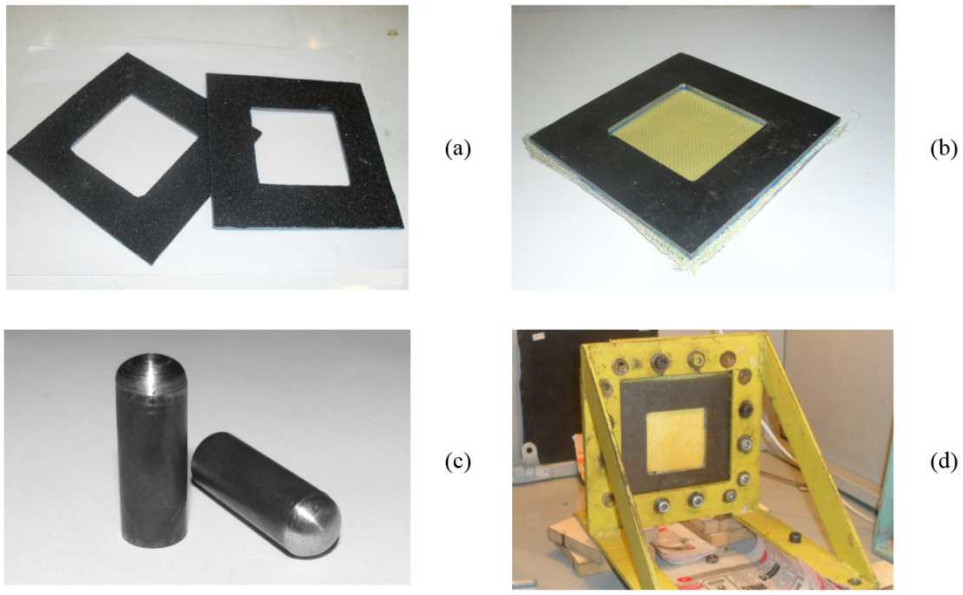

Fig. 3 High velocity impact test (a) Sandpaper on both sides of specimens within framework, (b) Framework, (c) Projectile and (d) Steel fixture for holding the fabric inside the framework.

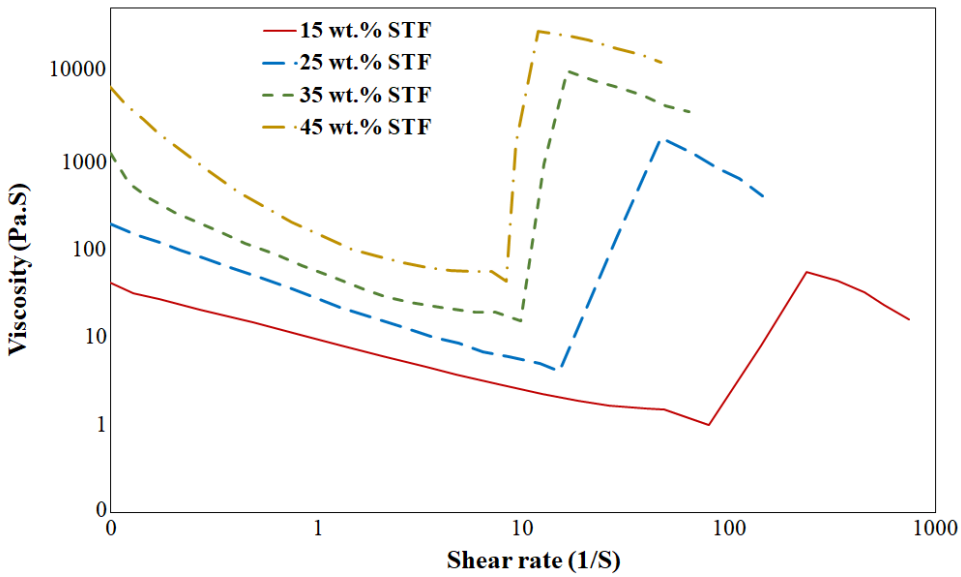

Fig. 4 Rheological behavior of STF made from polyethylene glycol (PEG) and nanosilica.

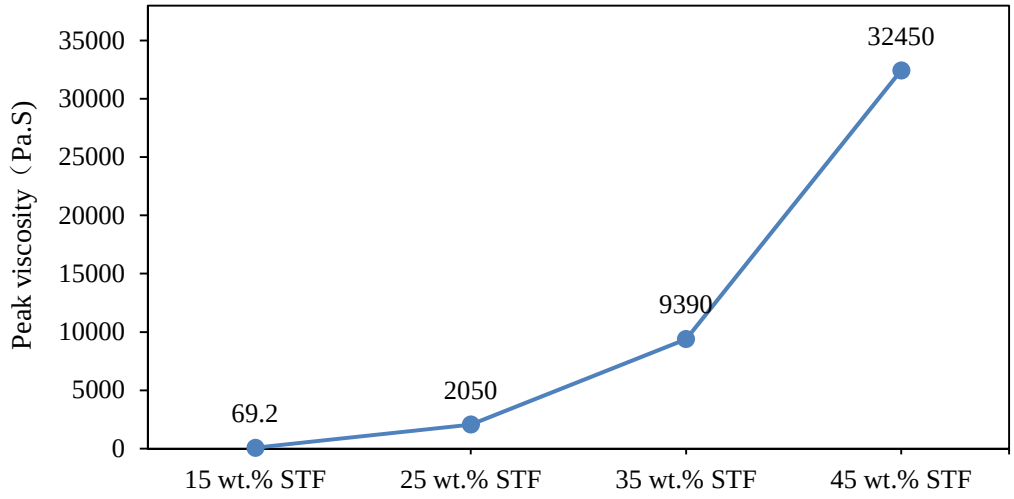

Fig. 5 Peak value of viscosity for STFs with different nanosilica loading.

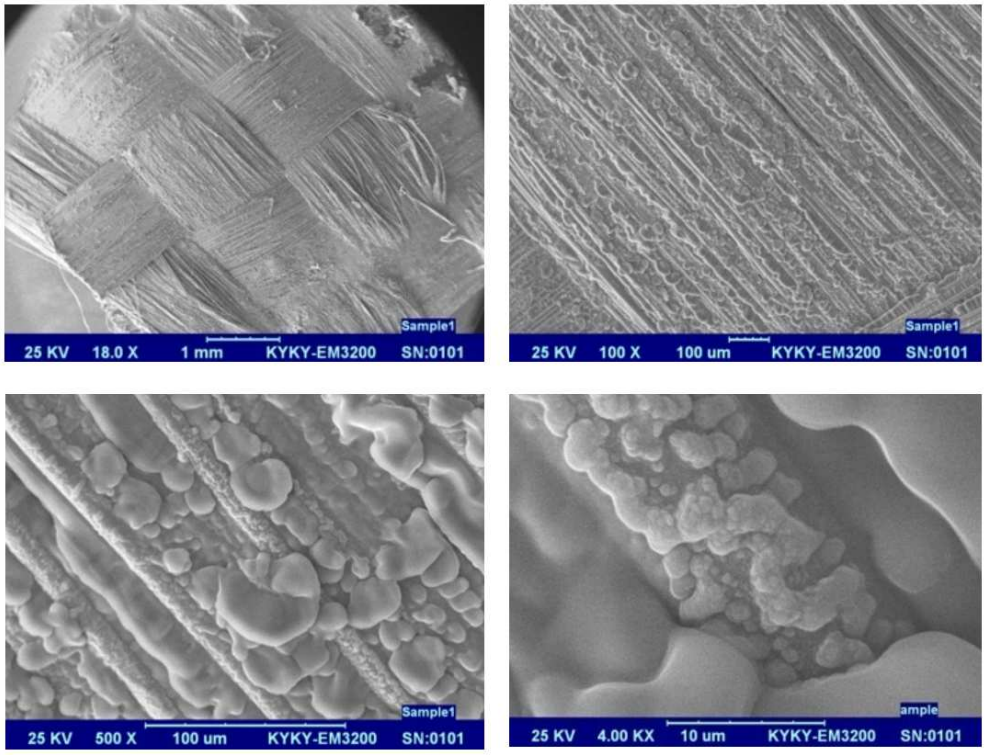

Fig. 6 Scanning electron microscopy (SEM) images of Kevlar fabric impregnated with 35 wt. % STF at: (a) ×18; (b) ×100; (c) ×500; (d) ×4000 magnifications.

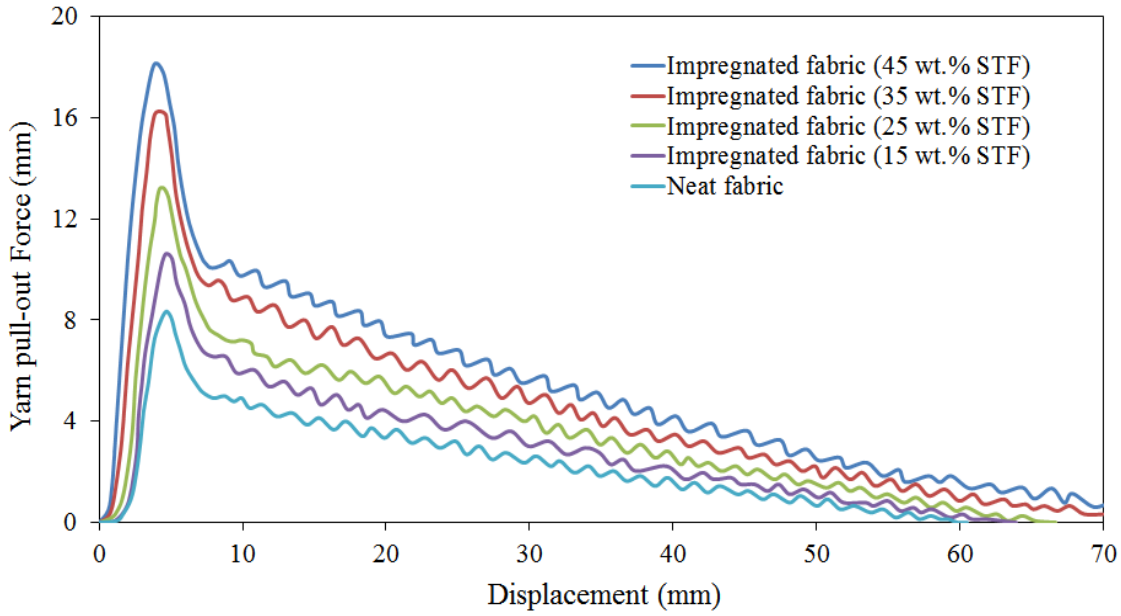

Fig. 7 Single yarn pull-out force versus displacement curve.

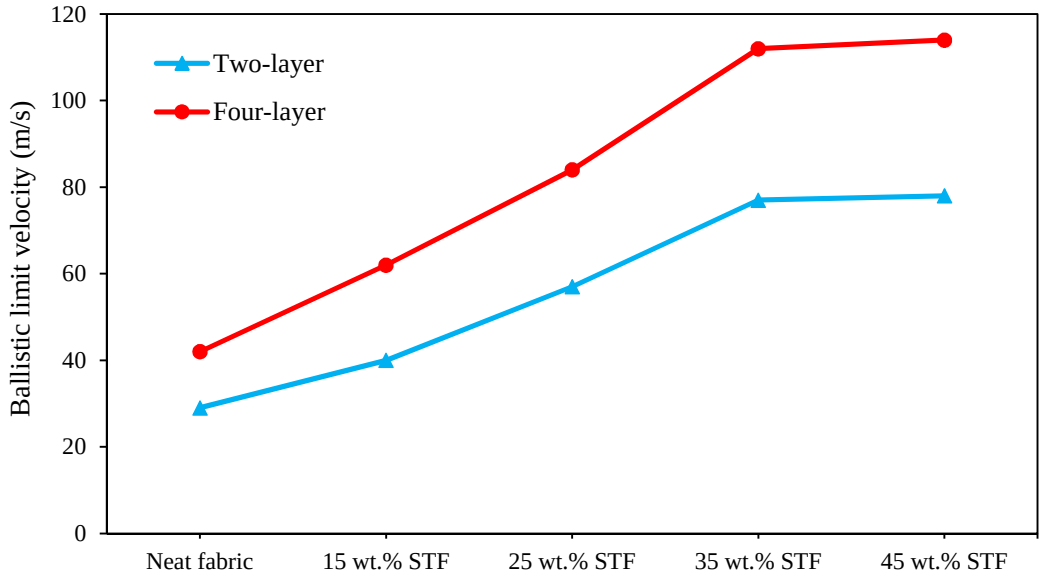

Fig. 8 Ballistic limits of two and four layer neat and impregnated fabrics with different nanosilica loading.

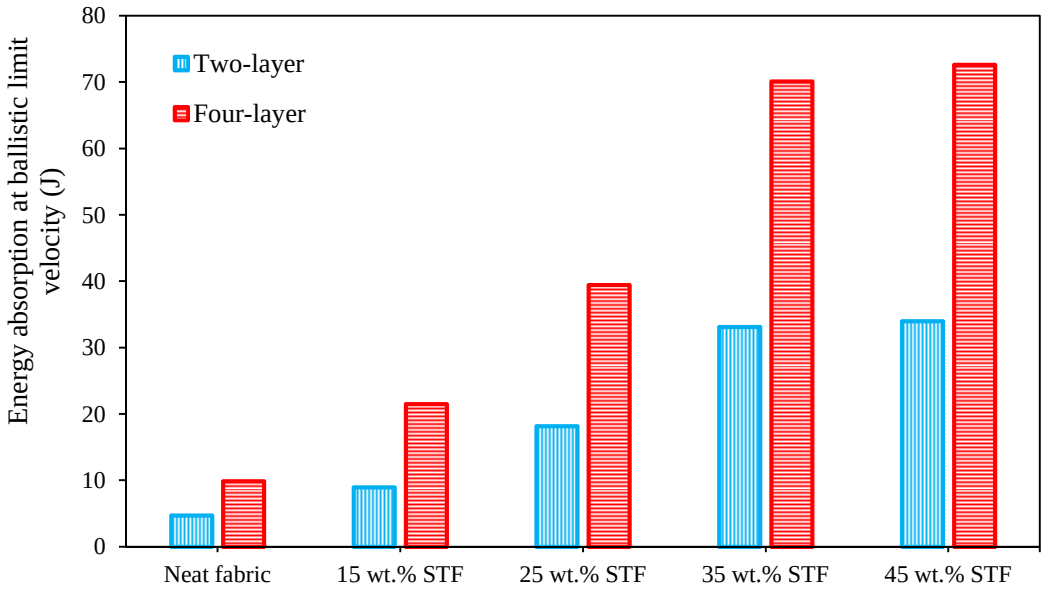

Fig. 9 Energy absorption of two and four layer samples.

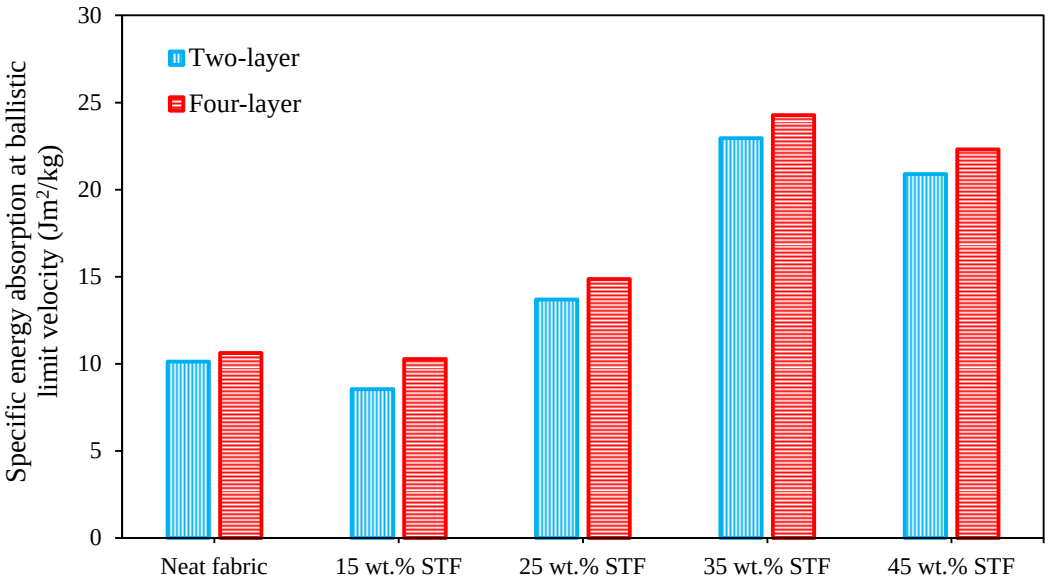

Fig. 10 Specific energy absorption (SEA) of two and four layer samples.

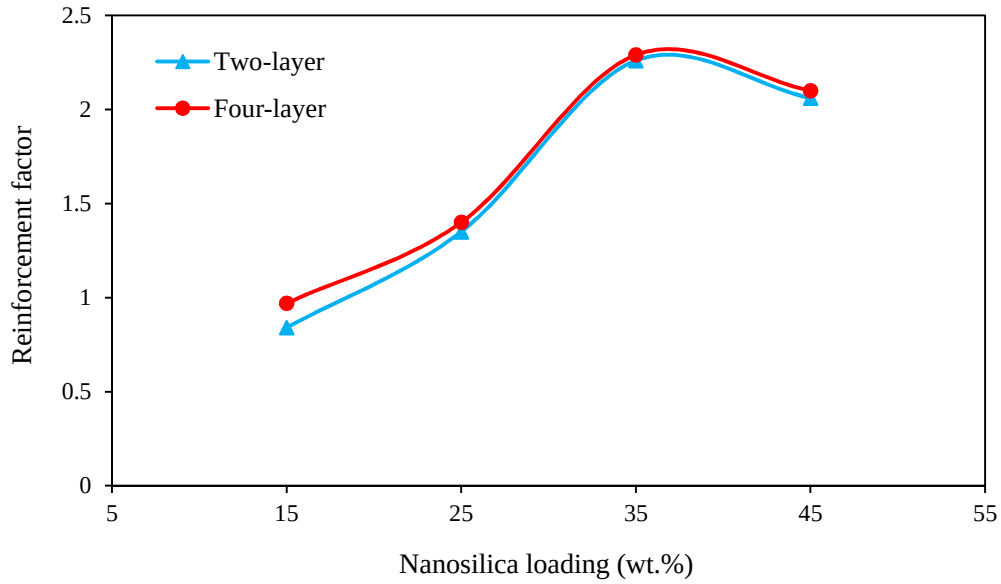

Fig. 11 Reinforcement factor of impregnated fabrics compared to the neat fabric.

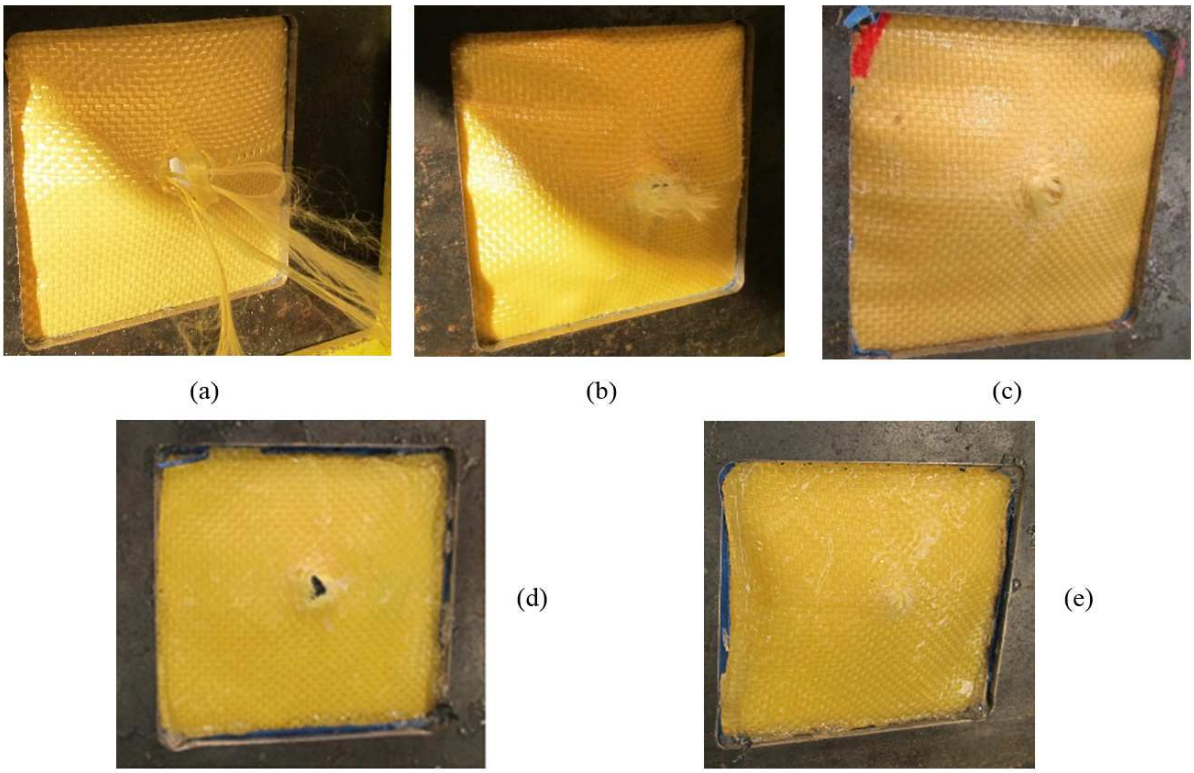

Fig. 12 Panels in high velocity impact tests. (a) Neat fabric (b) Impregnated fabric with 15 wt. % STF (c) Impregnated fabric with 25 wt. % STF (d) Impregnated fabric with 35 wt. % STF (e) Impregnated fabric with 45 wt. % STF.